Th 11 12

Improved Resolution Salt Imaging from 3D CSEM Anisotropic Inversion

J.P. Morten* (ElectroMagnetic GeoServices ASA), C. Twarz (ElectroMagnetic GeoServices ASA), V. Valente Ricoy-Paramo (ElectroMagnetic GeoServices ASA) & S. Sun (ElectroMagnetic GeoServices ASA)

SUMMARY

We present 3D CSEM imaging results for a Gulf of Mexico salt diapir. The dense receiver grid acquisition combined with a new approach to incorporate realistic electrical anisotropy in CSEM inversion leads to a detailed salt image. We compare to interpretations from 3D seismic, and show how information from the 3D CSEM data can be used to refine the salt structural interpretation.

Introduction

Salt diapirs are encountered in many of the world's most active areas for hydrocarbon exploration. The flanks of such structures are often considered prospective, and are therefore important geophysical imaging targets. However, imaging and interpretation of the salt-body geometry using seismic data alone can be challenging and requires advanced approaches both in acquisition and processing.

Non-seismic methods offer complementary structural information and have been successfully applied for salt imaging. For recent examples, see Hokstad *et al.* (2011) and Ceci *et al.* (2012). These authors consider 2D lines of controlled-source electromagnetic (CSEM) and magnetotelluric (MT) data, as well as full tensor gradient gravity data. Dense 3D grid acquisition of CSEM data gives further possibility to improve imaging resolution. Moreover, CSEM data are not fundamentally limited to low frequencies in deep water. This is the case for MT, which relies on naturally generated source signals that are attenuated in the water column.

In this paper, we consider anisotropic 3D CSEM inversion of deep water survey data recently acquired in the Gulf of Mexico. A dense receiver grid and an optimized source waveform were applied, and gives detailed reconstruction of the salt diapir. We compare the imaging results to the seismic interpretations, and demonstrate how the 3D CSEM imaging can lead to an updated salt interpretation and insight into the composition of salt and the degree of heterogeneity. This information allows enhanced understanding of the three dimensional arrangement of salt bodies, and finally prospect generation since the main play type for this area is three-way closure against salt bodies. We utilized a new regularization approach which allows incorporating *a priori* information about electrical anisotropy which significantly improves the geometrical definition of the salt body.

Gulf of Mexico salt diapir imaging

As part of an extensive 3D CSEM acquisition campaign in the Gulf of Mexico (Alcocer *et al.*, 2012), the survey considered here targeted a salt diapir with potential hydrocarbon reservoirs at the flanks. The survey objectives involved both the use of CSEM as a hydrocarbon indicator as well as structural imaging application. In this paper we will consider the salt structural imaging problem.

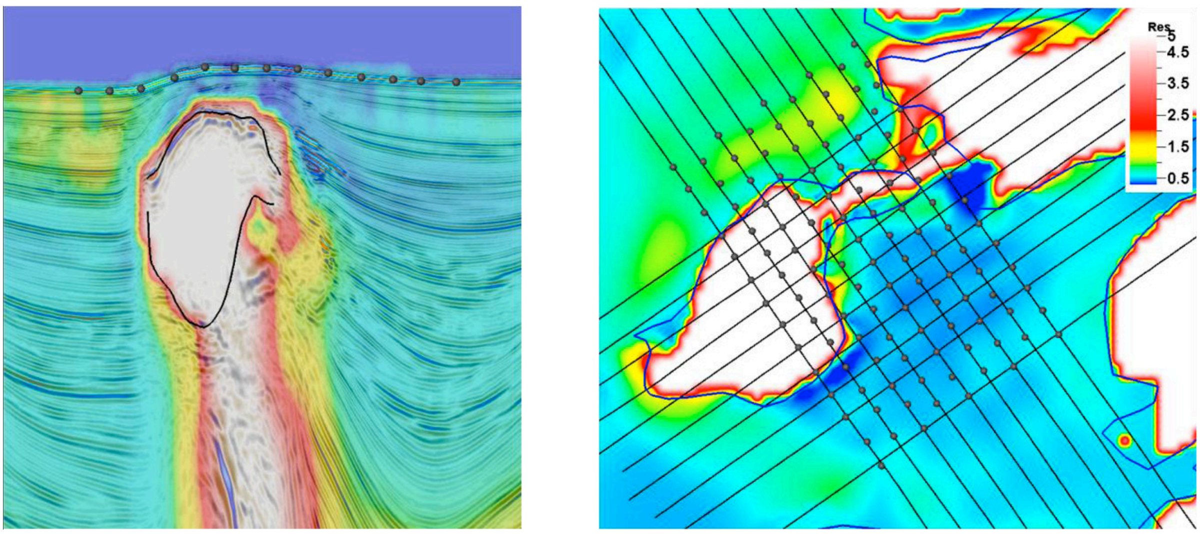

Figure 1 *The left image shows the result of the 3D CSEM inversion overlain with 3D seismic. The vertical resistivity component is shown; the black lines represent the salt top and base interpreted from seismic. The right image shows the survey layout where grey circles indicate receiver positions, and lines indicate source towlines. The top salt outline interpreted from seismic is shown as dark blue lines. The overlay shows a horizontal cross-section of the resistivity at 2000 m bmsl.*

The CSEM survey layout contained 125 receiver positions with spacing of 750 m, and 20 source towlines in a 3D grid survey configuration (Figure 1). All receivers were recording during the towing of all transmission lines, producing a complete 3D CSEM dataset, with significant azimuthal data coverage. The horizontal electric dipole source transmitted a composite waveform with a base frequency of 0.25 Hz, and a maximum current of 1250 A. The frequencies with largest power were 0.25, 0.5, 0.75 and 1.0 Hz. The water depth in the survey area ranges from 950 to 1450 m. From 3D seismic, several salt bodies were identified that can serve as structural traps for possible hydrocarbons in this area.

A robust initial resistivity model for 3D CSEM anisotropic inversion was established through analysis of well logs, seismic, and CSEM data. The model is defined by a vertical and a horizontal resistivity grid (TIV anisotropy). Salt bodies based on seismic data interpretation were included in the initial model to enhance convergence in inversion. All CSEM receiver data, comprising of inline and wide azimuth data were included in the inversion.

Figures 1 and 2 show our final inverted resistivity model. The data fit to the survey data for this model is on the scale of the measurement uncertainty. The 3D CSEM inversion result shows a salt root which was not previously mapped based on seismic data alone (Figures 1 and 2). In addition, the geometry of the salt flank varies in places significantly from the original interpretation, changing the prospectivity of the salt flank. From Figure 1 (left) it is obvious that the overhang of the salt is partially larger. The horizontal cross-section of the inversion result (Figure 1, right) indicates a connection in the North-East between the two main salt bodies in the survey area. Note that from the original seismic interpretation, they were separate bodies. The resistivity within the central salt body, as well as between the different salt bodies in the survey area varies significantly. This information received from CSEM inversion can help to understand the composition and internal structure of salt, *e.g.* higher clay content in pinch-out structures and in the salt root

Inclusion of *a priori* information about anisotropy was important in order to obtain the imaging results discussed above. The salt body shown in Figure 1 has approximately equal horizontal and vertical resistivity, i.e. it is recovered as electrically isotropic. This is in agreement with the expected resolution from inversion of CSEM data. The signals propagating in the salt vary over long length scales (*e.g.* the skin-depth, which is more than 1.5 km at 1 Hz in 10 Ωm). The inversion will recover an effective medium description of the salt, and at these long length-scales we expect the internal structure of the salt to be chaotic due to the salt migration process. The effective medium description for an unorganized medium should be isotropic. However, due to the vector nature of electromagnetic fields, a significant sensitivity difference between the horizontal and vertical electrical resistivity can lead to a strongly anisotropic representation of the salt body from anisotropic inversion. We explain in the next section how we introduced a new regularization to impose the *a priori* information that the salt body should be isotropic, and how this gives a significant improvement of the salt structural reconstruction.

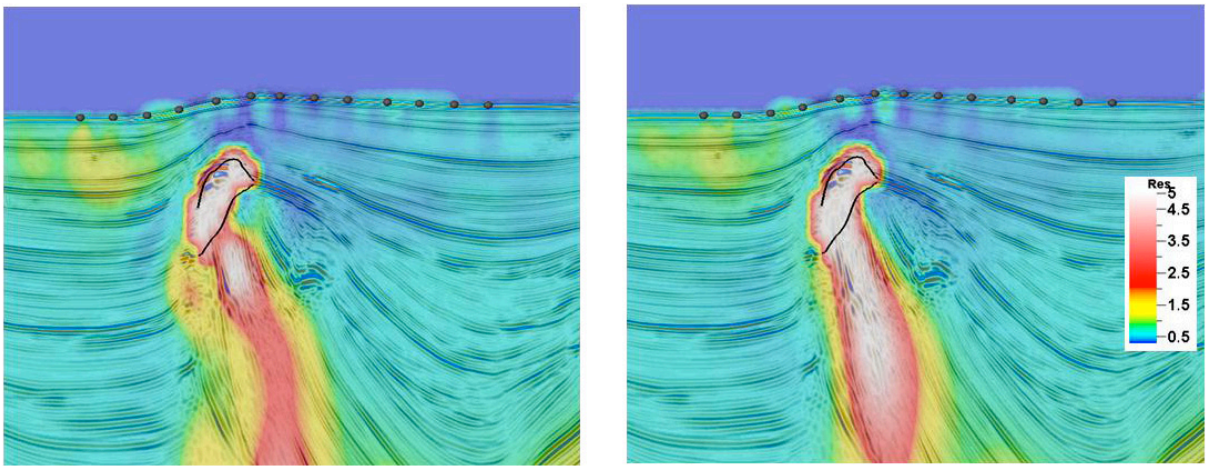

Figure 2 *We compare anisotropic 3D CSEM vertical resistivity resulting from inversion without regularizing the anisotropy ratio (left), and using the a priori anisotropy regularization function in Eq. (1) (right). The black lines represent the salt top and base interpreted from seismic. These results indicate how the additional information contributed by the regularization leads to an improved structural reconstruction without sensitivity artefacts in the vertical resistivity model.*

A priori anisotropy regularization

The vertical electric field component generated by the CSEM horizontal electric dipole source is essential in context of hydrocarbon exploration. Due to the boundary conditions at the resistive interface, a strong interaction with even very thin horizontal resistors will be effective, and give sensitivity to the presence of a hydrocarbon reservoir. Such responses can be fitted in inversion by introducing an anomalous resistivity into the vertical resistivity only. For a sufficiently thin resistor, the inversion does not need to introduce a contrast in the horizontal resistivity to fit the responses. This is because of the negligible interaction with the horizontal electric field at the thin resistor. It is the azimuth data available from 3D data which are associated with dominantly horizontal electrical fields. In 3D anisotropic inversion, additional geometrical information can be derived from such an absence of a response if we can incorporate *a priori* information on the anisotropy ratio $R=\rho_V/\rho_H$. As shown by Morten, Bjørke, and Nguyen (2010), if a regularization cost is associated with a large R then a thin resistor must be recovered with a more accurate vertical resolution when 3D CSEM data is inverted.

Similar to the thin resistor example, also isotropic resistors that are thick in the vertical direction may be associated with very different reconstructions into the vertical and horizontal resistivity. In this case, the interface interaction contribution due to vertical electric field boundary conditions may overwhelm response contributions that carry geometrical information about the resistor thickness. This interface interaction does not impact the broadside data from azimuth receivers in 3D CSEM. But in contrast to the thin resistor example, a thick resistive body will significantly impact the broadside data by interaction with the horizontal electrical field. In anisotropic inversion, such a body will typically be recovered as a thin-layered resistor in the vertical resistivity and as an extended body with more accurate thickness resolution in the horizontal resistivity. These reconstructions are characterized by a large R at the top interface and a small $R<1$ below.

If *a priori* information on the anisotropy ratio is available, we can obtain more accurate inversion results by imposing that information using regularization. We have implemented the following regularization function in the anisotropic 3D inversion,

$$\varepsilon_{\text{a.p. aniso}} = \sum_{i,j,k} \frac{W_{i,j,k}}{N_{\text{cells}}} \left[\Theta\left(R^{\text{lower}}_{i,j,k} - R_{i,j,k}\right) \left(\alpha \ln \frac{R_{i,j,k}}{R^{\text{lower}}_{i,j,k}}\right)^2 + \Theta\left(R_{i,j,k} - R^{\text{upper}}_{i,j,k}\right) \left(\ln \frac{R_{i,j,k}}{R^{\text{upper}}_{i,j,k}}\right)^2 \right] \qquad (1)$$

Here *i,j,k* are indices for the cells of the 3D model grid, $W_{i,j,k}$ is a weight grid, N_{cells} is the number of cells to be updated by the inversion, α is a scalar, and Θ is the Heaviside step function. The regularization cost of surpassing the upper (R^{upper}) or lower (R^{lower}) *a priori* anisotropy ratio bounds scales with the logarithm of the ratio between the actual value and the bound. Compared to the *a priori* anisotropy regularization introduced by Morten, Bjørke, and Nguyen (2010), this function treats a low value of R in a symmetric manner in relation to a high value of R: The logarithmic scaling ensures that as $R/R^{\text{lower}} \rightarrow 0$, the regularization cost becomes very large, similar to the case $R/R^{\text{upper}} \rightarrow \infty$. The parameter α allows to control the regularization cost growth-rate in the finite interval $0 < R \leq R^{\text{lower}}$.

The inversion results shown in Figure 2 demonstrate the impact of the *a priori* anisotropy regularization. The salt diapir is recovered with a realistic anisotropy, and the geometry is improved when the *a priori* anisotropy regularization is utilized. The additional information acts as a constraint that allows the inversion to consistently reconstruct more details of the salt-diapir from the data.

Conclusions

We have demonstrated how 3D CSEM data can aid exploration by improved imaging of salt flanks and base salt geometries. The obtained anisotropic inversion results are compared to 3D seismic, and we discuss the implications of the updated interpretation. Since salt is expected to be nearly electrically isotropic on the length-scales of the measurement, we introduced a new regularization function to mitigate the sensitivity difference between horizontal and vertical resistivity components. This regularization enforces that the salt body geometry is reconstructed realistically in both the vertical and horizontal components of resistivity, and improves definition of geometrical details. Our imaging results demonstrate that CSEM data has the potential to enhance interpretation in complex salt affected areas. Incorporation of the obtained resistivity data into seismic velocity model building workflows can also enhance the fidelity and resolution of seismic sub-salt imaging.

Acknowledgements

The authors thank PEMEX and EMGS for the possibility to present this work.

References

Alcocer, J., García, M., Soto, H., Roth, F., Baltar, D., Gabrielsen, P., and Paramo, V. (2012) Experience from using 3D CSEM in the Mexican deepwater exploration program. SEG Technical Program Expanded Abstracts 2012:pp. 1-5.

F. Ceci, A. Lovatini, L. Masnaghetti, K. Hokstad and V. Antonsdottir (2012), Multi Measurement Imaging Using Seismic CSEM MMT and FTG Data for Salt Dome Evaluation in the Nordkapp Basin, 74th EAGE Conference & Exhibition, B034.

Hokstad, K., Fotland, B., Mackenzie, G., Antonsdottir, V., Foss, S., Stadtler, C., Fichler, C., Haverl, M., Waagan, B., Myrlund, E., Masnaghetti, L., Ceci, F., and Raya, P. (2011) Joint imaging of geophysical data: Case history from the Nordkapp Basin, Barents Sea. SEG Technical Program Expanded Abstracts 2011: pp. 1098-1102.

Morten, J., Bjørke, A., and Nguyen, A. (2010) Hydrocarbon reservoir thickness resolution in 3D CSEM anisotropic inversion. SEG Technical Program Expanded Abstracts 2010: pp. 599-603.